

Model for the thickness dependence of electron concentration in InN films

V. Cimalla,^{a)} V. Lebedev, and F. M. Morales

Institute for Micro- and Nanotechnologies, Technical University Ilmenau, Kirchhoffstr. 7, 98693 Ilmenau, Germany

R. Goldhahn

Institute for Micro- and Nanotechnologies, Technical University Ilmenau, Kirchhoffstr. 7, 98693 Ilmenau, Germany and Institute of Physics, Technical University Ilmenau, P.O. BOX 100565, 98684 Ilmenau, Germany

O. Ambacher

Institute for Micro- and Nanotechnologies, Technical University Ilmenau, Kirchhoffstr. 7, 98693 Ilmenau, Germany

(Received 13 February 2006; accepted 7 September 2006; published online 24 October 2006)

A model for the influence of different contributions to the high electron concentration in dependence on the film thickness of state-of-the-art InN layers grown by molecular-beam epitaxy is proposed. Surface accumulation has a crucial influence for InN layers <300 nm and superimposes the background concentration. For air-exposed InN, it can be assigned to a surface near doping by oxygen. For InN layers in the micron range the density of dislocations is the major doping mechanism. Finally, point defects such as vacancies and impurities have minor influence and would dominate the free electron concentration only for InN >10 μm . © 2006 American Institute of Physics. [DOI: 10.1063/1.2364666]

Indium nitride is a low-band-gap material, which received an increasing attention over the last years due to its very prospective properties. In particular, the high electron mobility¹ should predestine the material for high frequency devices. A major drawback, however, is the high electron concentration in InN layers, which up to date prevents the development of any kind of electronic device. Despite of the remarkable progress in the growth of InN by different techniques [plasma-induced molecular-beam epitaxy^{2,3} (pi-MBE) and metal organic chemical vapor deposition⁴], all layers appear to be degenerated with electron concentrations higher than 10^{17} cm^{-3} and the exact mechanisms of its origin are still under debate. Generally, the electron concentration n decreases with increasing thickness th by $n \sim th^{-\alpha}$, however, with a nonconstant slope² $\alpha < 1$ indicating the superposition of several n -type doping mechanisms. The possible contributions to the apparent electron concentration can be classified by three models: (i) a localized electron accumulation with specific sheet carrier concentration $N_{S,0}$ (i.e., $\alpha=1$), (ii) a homogeneous background volume concentration n_b (i.e., $\alpha=0$), and (iii) an inhomogeneous carrier distribution n_{inhom} over the InN film (i.e., α depends on the mechanism). Consequently, the net electron density in dependence on the InN film thickness th will be

$$n = \frac{1}{th} N_{S,0} + n_b + \frac{1}{th} \int_0^{th} n_{\text{inhom}} dz. \quad (1)$$

The aim of this work is to model the influence of the different doping mechanisms in dependence of the layer thickness for MBE-grown InN films. In particular, the influence of threading dislocations (TDs) for an inhomogeneous doping will be demonstrated. The InN layers were grown⁵ in a BALZERS MBE system using conventional effusion cells for In, Ga, and Al and a rf nitrogen plasma source. First, an

AlN buffer layer was grown by a two-step procedure. The growth was initiated by nitridation at $\sim 1100^\circ\text{C}$ for 2 min, and at $\sim 900^\circ\text{C}$ AlN templates were prepared in a two-dimensional mode with a thickness of about 200–300 nm. All InN epilayers were grown at $\sim 380^\circ\text{C}$ under stoichiometric (1:1) conditions to prevent surface metal accumulation. The growth process was monitored by a digitized pattern of reflection high-energy electron diffraction. The thickness of the InN layer has been varied from 0.07 to 2.2 μm . The electron concentration was determined by Hall measurements at 0.4 T in van der Pauw geometry. Samples of $5 \times 5 \text{ mm}^2$ were processed by conventional photolithography to form In point contacts with a spacing of 5 mm for Hall measurements. The contacts were annealed at 150°C . It should be noted that the electron concentration for inhomogeneous samples measured by Hall is not the pure addition as in Eq. (1). It rather should be weighted by the electron mobility. Due to the lack of reliable data, we used this simplification where an error of up to 20% can be expected.

Microstructural analysis was performed by transmission electron microscopy (TEM) with an accelerating voltage of 200 kV. The TD density was estimated by a digital imaging processing of cross sectional TEM micrographs and confirmed by the analysis of a series of plan view TEM micrographs taken at samples with different InN film thickness.⁵ The resulting TD density in dependence on the distance to the interface to the AlN buffer layer is shown in Fig. 1. Here, we do not differentiate between edge, screw, and mixed dislocations. More details about the growth procedure and the structural and electronic characterization can be found elsewhere.⁵

The apparent carrier concentration is decreasing with increasing film thickness similar to the most extensive studied series of InN films available in the literature, which was taken as reference. These InN films were also grown by pi-

^{a)}Electronic mail: volker.cimalla@tu-ilmenau.de

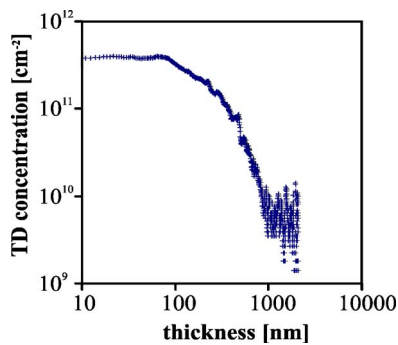


FIG. 1. Density of threading dislocations in a $2.2 \mu\text{m}$ thick InN in dependence on the distance to the AlN–InN interface (Ref. 5).

MBE on sapphire with AlN or AlN/GaN buffer layers^{2,6,7} and show very similar electronic properties (for the electron concentration see Fig. 2, for mobility see Ref. 5), which implies the same underlying doping mechanism. Moreover, for thicker layers the determined TD density shows a good agreement with previous TEM studies⁸ performed on the samples of Lu *et al.*,² where a TD density of $2.2 \times 10^{10} \text{ cm}^{-3}$ was estimated for 760 nm InN layers grown on a GaN/AlN buffer.

Lu *et al.*⁶ observed such a strong reduction of the electron concentration with increasing film thickness and concluded a high accumulation at the interfaces of about 4.3×10^{13} and $2.5 \times 10^{13} \text{ cm}^{-2}$ for InN layers grown on AlN and GaN buffer layers, respectively. By *C-V* depth profiling in electrolyte, a surface accumulation of $1.57 \times 10^{13} \text{ cm}^{-2}$ was estimated. This surface accumulation was discussed as an intrinsic property of InN due to the extraordinary low conduction band minimum at the Γ point,⁹ which allows donor-type surface states to be located inside the conduction band. As a consequence, Piper *et al.* estimated on clean InN surfaces prepared by an atomic hydrogen treatment¹⁰ a surface Fermi level of 1.58 eV (Ref. 9) to 1.64 eV (Ref. 11) above the valence band maximum, i.e., about 0.9–1.0 eV above the conduction band minimum, by high-resolution electron energy loss spectroscopy. The corresponding surface state density is about $2.4 \times 10^{13} \text{ cm}^{-2}$.

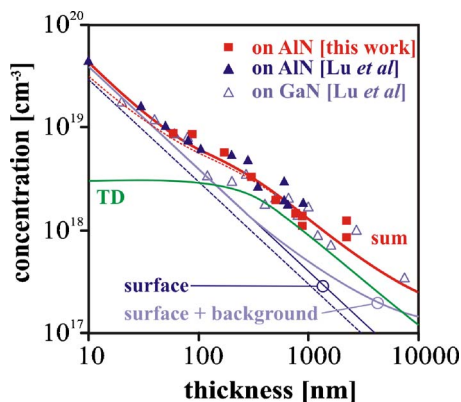


FIG. 2. Average electron carrier concentration in dependence on the InN film thickness on AlN buffer in comparison to the discussed models, where “surface” means the influence of a localized sheet carrier density of $4.3 \times 10^{13} \text{ cm}^{-2}$ at the surface (Ref. 6), “background” the influence of a fixed bulk concentration (Ref. 15) of $1 \times 10^{17} \text{ cm}^{-3}$, “TD” the contribution of threading dislocations, and “sum” the addition of all effects. Dashed lines represent InN on GaN/AlN buffer. For comparison, also the data of Lu *et al.* (Refs. 2 and 6) and Schaff *et al.* (Ref. 7) are shown; filled and open triangles represent InN on AlN and GaN/AlN buffers, respectively.

Recently we found a very similar surface electron concentration and Fermi level position on an air-exposed InN surface by *in situ* measurements of the resistance of an InN film during sputter depth profiling¹² and ultraviolet photoelectron spectroscopy,¹³ respectively. The depth profile of the electron concentration follows in a very good agreement the oxygen concentration close to the surface estimated by Auger electron spectroscopy.^{12,13} Moreover, an interface charge of about $5 \times 10^{12} \text{ cm}^{-2}$, localized at the interface between InN and the GaN buffer layer, was estimated^{12,14} and is expected to be even higher at the interface between InN and AlN.¹⁴ The sum electron accumulation on both interfaces is superimposing the bulk concentration for InN films of up to $7.5 \mu\text{m}$ (Ref. 7) and explains qualitatively the observed dependence of the electron concentration on the film thickness. It is characterized by a constant sheet carrier concentration $N_{S,0}$. Consequently the dependence of the volume concentration n on the thickness th must follow a linear law $n = N_{S,0}/th$ (Fig. 2, “surface”). For $N_{S,0}$ the already mentioned values achieved by extrapolating the measured sheet carrier concentration N_S of thin InN films to zero thickness as described by Lu *et al.*⁶ were used. Considering a surface accumulation of $2.2 \times 10^{13} \text{ cm}^{-3}$, which is independent of the buffer layer for thicker InN films, interface charges of 0.3×10^{13} and $2.3 \times 10^{13} \text{ cm}^{-3}$ at the interface to GaN and AlN, respectively, can be expected. The value for the GaN buffer layer is in good agreement with the sputtering experiments, which revealed an interface concentration of about $0.5 \times 10^{13} \text{ cm}^{-3}$. However, Fig. 2 clearly demonstrates that the apparent electron concentrations in this work (squares) as well as the data of Lu *et al.*⁶ cannot be fitted with a linear law $n = N_{S,0}/th$. The smaller slope indicates the contribution of an additional, inhomogeneous doping mechanism.

The inhomogeneous electron distribution in InN layers was analyzed by Swartz *et al.* using variable-magnetic-field Hall measurements.^{16,17} In addition to a part of carriers with low mobility and high density, which can be attributed to the surface accumulated layer, the values for the bulk carriers were extracted. Both bulk mobility and electron concentration are still depending on the layer thickness for InN films with a total thickness of up to about $1 \mu\text{m}$. For a thick film on GaN/AlN buffer ($7.5 \mu\text{m}$), a background carrier concentration of $1 \times 10^{17} \text{ cm}^{-3}$ was estimated. For its origin several effective donors are possible. Both oxygen¹³ and hydrogen¹⁸ have shown to create donor states inside the conduction band and for oxygen an effective doping efficiency of more than 50% was observed.^{12,13} However, elementary analysis by secondary ion mass spectroscopy revealed a background concentration of oxygen, hydrogen, and carbon to be in the 10^{16} cm^{-3} range, i.e., two to ten times smaller than the electron concentration.⁷ Similar to surface states,¹⁹ intrinsic defects such as point defects and dislocations are expected to create donor states inside the conduction band. As a typical point defect, vacancies were investigated by positron annihilation spectroscopy by Oila *et al.*²⁰ N vacancies were found to be the dominating type with a concentration, which is about one order of magnitude lower than the electron concentration. All these effects can be summed up to the background concentration of $1 \times 10^{17} \text{ cm}^{-3}$ estimated by variable-magnetic-field Hall measurements on GaN/AlN buffer.^{16,17} The influence of both surface accumulation and background concentration is shown in Fig. 2 by the curve “surface + background.”

On the other side, the density of dislocations in heteroepitaxial layers is typically monotonically decreasing with the layer thickness,⁸ and the influence of these defects explains qualitatively the dependence of the background carrier concentration on the layer thickness within the first 1 μm .¹⁶ For quantification, it is assumed that each dislocation creates donors with a specific distance in the growth direction. Using the concentration profile of Fig. 1, its influence is shown in Fig. 2. Similar to the TD density (Fig. 1), the concentration of the electrons from the TDs only (“TD”) starts to decrease at a thickness of about 100 nm. For the sum of all the discussed effects (“sum”), a very good agreement with the measured data is achieved if the distance in growth direction is about 1.14 nm, i.e., if in a TD only every second InN unit cell bears an effective donor or only 50% of the dislocations are active. In contrast to GaN,²¹ the underlying doping mechanisms of dislocations are not investigated and require further analysis. Taking the similarities of the materials into account, in particular, the dominating edge dislocations⁵ are creating vacancies. Previously these vacancies have been expected to be negatively charged.^{22,23} However, in contrast to GaN, the branch point energy E_B at the Γ point in InN is located deep inside the conduction band.⁹ Intrinsic defects are charged in a way to shift the Fermi level E_F towards E_B . Consequently, in n -type GaN where $E_F > E_B$, the vacancies are negatively charged, while in InN, where $E_F < E_B$, such defects should be positively charged, i.e., a donor-type behavior can be expected. The observed dependence of the electron concentration on the InN film thickness confirms this assumption, since for InN in the micron range the measured concentration is higher than the sum of all other possible contributions.

In conclusion, for state-of-the-art MBE-grown InN, three major mechanisms determine the apparent electron concentration on different thickness scales. First, the accumulation of electrons at the surface and the interface clearly dominates the electronic properties of InN for thin layers with $th < 300$ nm. For nondegenerate InN, an electron concentration below 10^{17} cm^{-3} would be necessary and already the accumulation layers would prevent to achieve this for InN films of up to $\sim 5 \mu\text{m}$. Second, layers in the micron range are strongly affected by threading dislocations. Finally, the background concentration of InN is already well controlled and would influence the apparent carrier concentration only for films with $th > 10 \mu\text{m}$. However, the influence of such point defects might have substantial influence on the mobility. As a consequence, for an application of InN films for electronic devices, both the reduction of the density of threading dislo-

cations and the suppression of the electron accumulation at the interfaces are of crucial importance.

This work was supported by the Thuringian Ministry of Culture (TKM) and the European Union (B509-04011, EFRE Program: B 678-03001, and 6th Framework Program: GaNano NMP4-CT2003-505614).

- ¹V. M. Polyakov and F. Schierz, *Appl. Phys. Lett.* **88**, 032101 (2006).
- ²H. Lu, W. J. Schaff, L. F. Eastman, J. Wu, W. Walukiewicz, D. C. Look, and R. J. Molnar, *Mater. Res. Soc. Symp. Proc.* **743**, L4.10 (2003).
- ³E. Dimakis, E. Illiopoulos, K. Tsagaraki, Th. Kehagias, Ph. Kominou, and A. Georgakilas, *J. Appl. Phys.* **97**, 113520 (2005).
- ⁴A. Yamamoto, T. Tanaka, K. Koide, and A. Hashimoto, *Phys. Status Solidi B* **194**, 510 (2002).
- ⁵V. Lebedev, V. Cimalla, T. Baumann, P. Morales, and O. Ambacher, *J. Phys. Chem. Solids* (to be published).
- ⁶H. Lu, W. J. Schaff, L. F. Eastman, and C. E. Stutz, *Appl. Phys. Lett.* **82**, 1736 (2003).
- ⁷W. J. Schaff, H. Lu, L. F. Eastman, W. Walukiewicz, K. M. Yu, S. Keller, S. Kurtz, B. Keyes, and L. Gevilas, *Proc.-Electrochem. Soc.* **2004-06**, 358 (2004).
- ⁸C. J. Lu, L. A. Bendersky, H. Lu, and W. J. Schaff, *Appl. Phys. Lett.* **83**, 2817 (2003).
- ⁹I. Mahboob, T. D. Veal, L. F. J. Piper, C. F. McConville, H. Lu, W. J. Schaff, J. Furthmüller, and F. Bechstedt, *Phys. Rev. B* **69**, 201307 (2004).
- ¹⁰L. F. J. Piper, T. D. Veal, I. Mahboob, C. F. McConville, H. Lu, and W. J. Schaff, *J. Vac. Sci. Technol. A* **23**, 617 (2005).
- ¹¹I. Mahboob, T. D. Veal, C. F. McConville, H. Lu, and W. J. Schaff, *Phys. Rev. Lett.* **92**, 036804 (2004).
- ¹²V. Cimalla, G. Ecke, M. Niebelschütz, O. Ambacher, R. Goldhahn, H. Lu, and W. J. Schaff, *Phys. Status Solidi C* **2**, 2254 (2005).
- ¹³V. Cimalla, M. Niebelschütz, G. Ecke, V. Lebedev, O. Ambacher, M. Himmerlich, S. Krischok, J. A. Schaefer, H. Lu, and W. J. Schaff, *Phys. Status Solidi A* **203**, 59 (2006).
- ¹⁴V. Cimalla, Ch. Förster, G. Kittler, I. Cimalla, R. Kosiba, G. Ecke, O. Ambacher, R. Goldhahn, S. Shokhovets, A. Georgakilas, H. Lu, and W. J. Schaff, *Phys. Status Solidi C* **0**, 2818 (2003).
- ¹⁵T. D. Veal, L. F. J. Piper, I. Mahboob, H. Lu, W. J. Schaff, and C. F. McConville, *Phys. Status Solidi C* **2**, 2246 (2005).
- ¹⁶C. H. Swartz, R. P. Tompkins, N. C. Giles, T. H. Myers, H. Lu, W. J. Schaff, and L. F. Eastman, *J. Cryst. Growth* **269**, 29 (2004).
- ¹⁷C. H. Swartz, R. P. Tompkins, T. H. Myers, H. Lu, and W. J. Schaff, *Phys. Status Solidi C* **2**, 2250 (2005).
- ¹⁸E. A. Davis, S. F. J. Cox, R. L. Lichti, and C. G. van der Walle, *Appl. Phys. Lett.* **82**, 592 (2003).
- ¹⁹C. G. van der Walle and J. Neugebauer, *Nature (London)* **423**, 626 (2003).
- ²⁰J. Oila, A. Kemppinen, A. Laasko, K. Saarinen, W. Egger, L. Liskay, P. Sperr, H. Lu, and W. J. Schaff, *Appl. Phys. Lett.* **84**, 1486 (2004).
- ²¹I. Arslan, A. Bleloch, A. A. Stach, and N. D. Browning, *Phys. Rev. Lett.* **94**, 025504 (2005).
- ²²J. S. Thakur, R. Naik, V. M. Naik, D. Haddad, G. W. Auner, H. Lu, and W. J. Schaff, *J. Appl. Phys.* **99**, 023504 (2006).
- ²³D. C. Look, H. Lu, W. J. Schaff, J. Jasinski, and Z. Lilienthal-Weber, *Appl. Phys. Lett.* **80**, 258 (2002).